Electronic Supplementary Material (ESI) for Physical Chemistry Chemical Physics.

Supplementary Information for:

Small Gold Clusters Catalyzing the Conversion of Glycerol to Epichlorohydrin

Anthony M. Pembere, Mengzhou Yang, Zhixun Luo*

State Key Laboratory for Structural Chemistry of Unstable and Stable Species, Institute of Chemistry, Chinese Academy of Sciences, Beijing 100190, China.
Email:zxluo@iccas.ac.cn

Contents

Experimental and Theoretical details.

Experimental and Theoretical details.

S1. Mass Spectrometric Analysis：

Figure S1 shows the high-resolution mass spectrum of Au_n cluster species synthesized by laser ablation in water, where the dominant peaks are assigned to $Au_5(H_2)^-$, $Au_5(H_3O)^-$, $Au_5(H_20)_{10}H_3^-$, $Au_{20}(H_30)_8(H_2)^-$ and $Au_4(H_20)_3(H_3O)^+H_3^+$.This is consistent with previous reports which have noted that the electrostatic effects can control agglomeration behaviour, enabling these metal hydration clusters to attach additional hydrogen atoms and the Rydberg atom (H_3O) is stable species in water. It is notable that the stability and electrostatic stabilization are experimentally associated with the use of N_2–gas in the preparation process since the convective current of nitrogen and water benefits thermal transmission, as well as separation distances among the gold clusters.

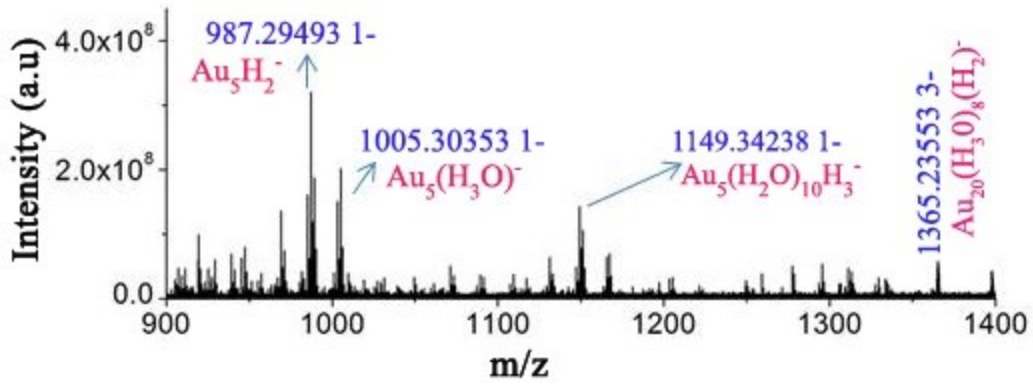

Figure S1.ESI-MS spectra of gold clusters obtained by laser ablation in water followed by filtration.

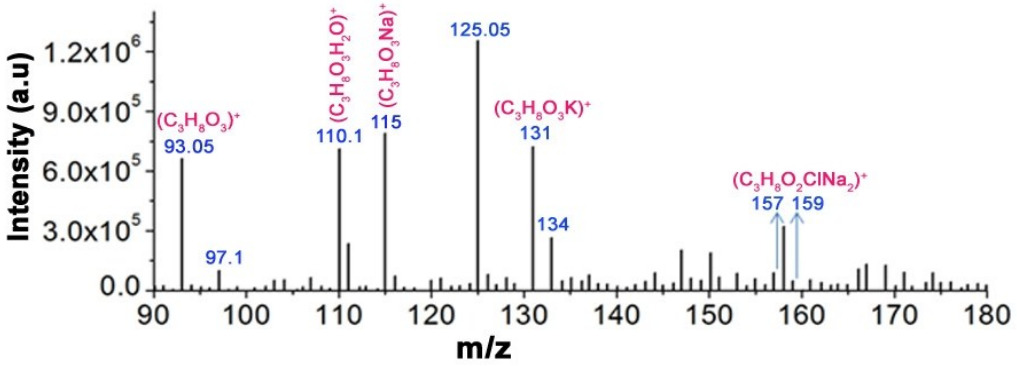

Figure S2. ESI-MS spectra (positive mode) glycerol without laser ablation at the presence of gold rod at the addition of 0.5 ml HCl (1M), as an exclusionexperiment.

S2. Structural Optimization and Energy calculation:

The Sum of electronic and zero point energies for the optimized structuresare calculated. The difference of total electronic and zero point energies (ΔE) was used to elucidate the reaction coordinates.DFT calculations of the reactants binding shows that both reactants (HCl and glycerol) prefer to co-bind on the Au cluster catalyst as it presents a relatively strong binding state as seen in figuresS3, S4, S5, S6.

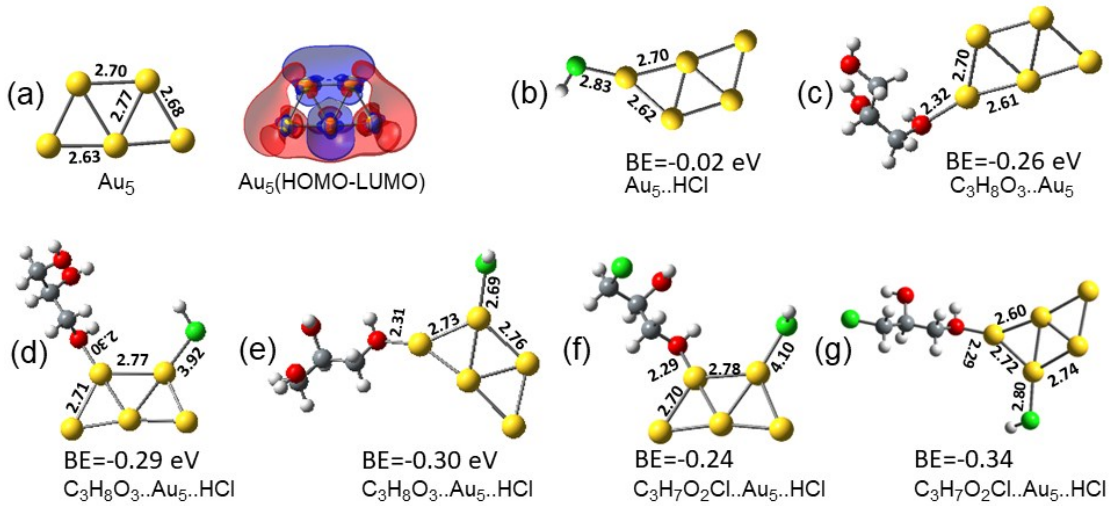

Figure S3. Optimized structures and binding energies of HCl-Au_5, Au_5-$C_3H_8O_3$, HCl-Au_5-$C_3H_8O_3$and HCl-Au_5-$C_3H_7O_2Cl$ complexes. Bond lengths are in angstroms. Atoms in yellow, red, grey, white, green colour represent Au, O, C, H and Cl respectively.

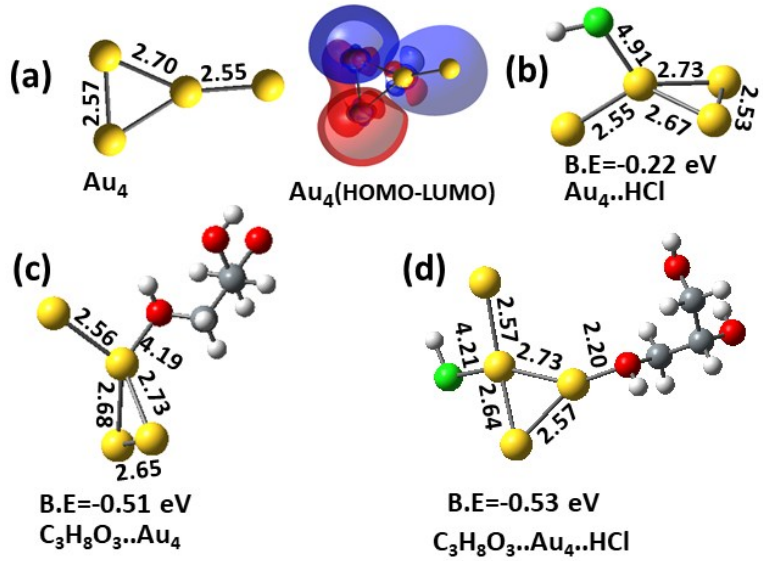

Figure S4. Optimized structures and binding energies of HCl-Au_4, Au_4-$C_3H_8O_3$ and HCl-Au_4-$C_3H_8O_3$ complexes. Bond lengths are in angstroms. Atoms in yellow, red, grey, white, green colour represent Au, O, C, H and Cl respectively.

S3. HOMO-LUMO gaps:

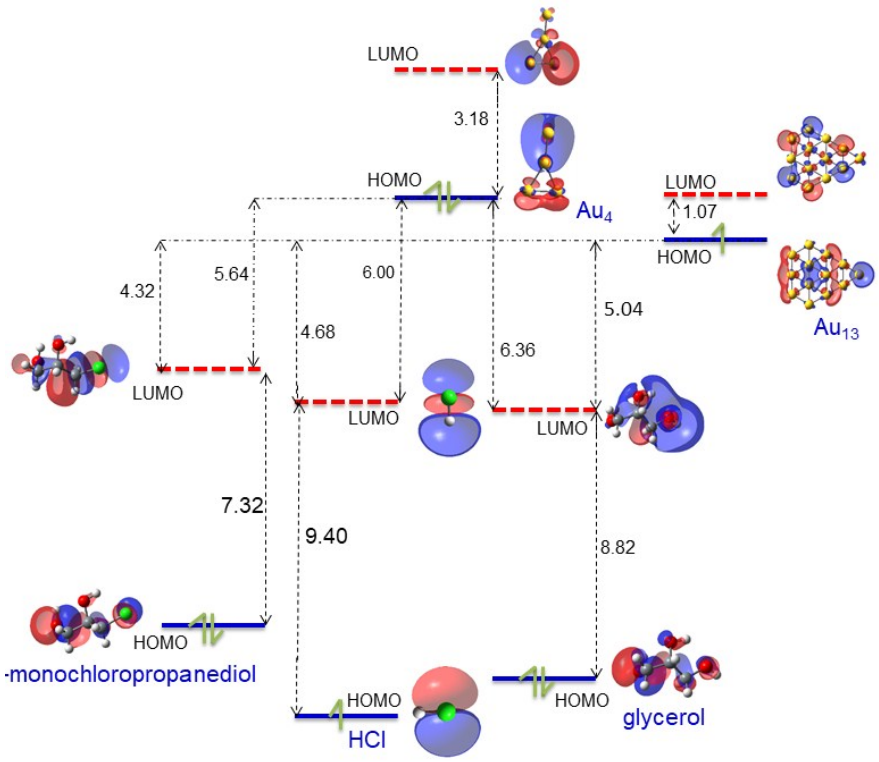

Figure S5. The HOMOs, LUMOs, and HOMO–LUMO gaps of glycerol, monochloropropanediol, HCl and Au_nclusters.Energies are in eV. Atoms in yellow, red, grey, white, green colour represent Au, O, C, H and Cl respectively.

S4. NBO Analysis:

Similar to the results for Au_5 as given in the main text, dominant donor-acceptor charge-transfer interaction are also checked out for the Au_4, alongside a summary of natural population analysis indicating natural charge and natural bond orbitals. Specifically, $LP_o \rightarrow LP_{Au}$(0.96 eV) is observed in HCl-Au_4–$C_3H_8O_3$complex (Figure S6). In comparison, we find $LP_O \rightarrow LP^*_{Au}$ (0.92 eV) and $LP_{Cl} \rightarrow LP^*_{Au}$ (0.36 eV) in $C_3H_7O_2Cl$-Au_4-HCl.

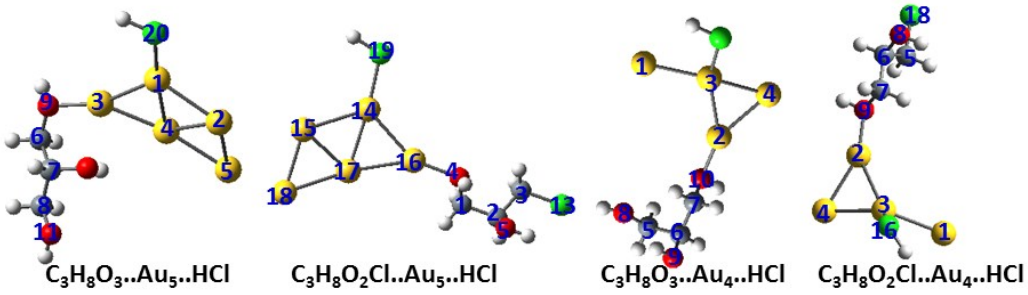

Figure S6. Atom labels for all the following analysis. Atoms in yellow, red, grey, white, green color represent Au, O, C, H and Cl respectively.

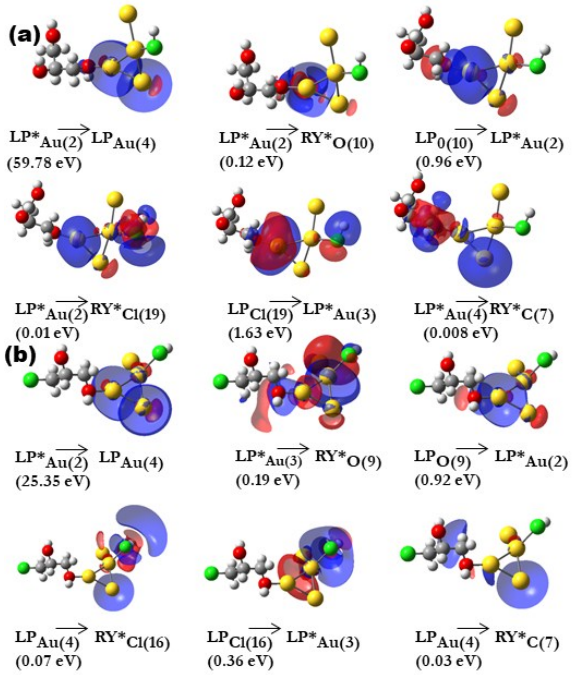

Figure S7. Second order perturbation theory analysis of Fock matrix in NBO donor–acceptor interactions in HCl-Au_4–$C_3H_8O_3$ **(a)**, and HCl-Au_4–$C_3H_7O_2Cl$ **(b)**. Atoms in yellow, red, grey, white, green color represent Au,O,C, H and Cl respectively.The inserts indicate atom numbers while BD (bonding orbital), BD* (antibonding orbital), LP (antibonding lone pair), RY (Rydberg orbital), RY* (Rydberg antibond) are molecular orbitals.

S5. Reaction Pathway for Au_4 Catalysis:

Bearing in mind that cluster properties are not only dependent on the electronic behaviours but also geometric structures, we have compared the dehydrochlorination reaction pathway along with planarAu_4, as shown in Figure S8.It is worth noting that Au_4 shows a higher binding energy (-0.53 eV) than Au_5. Also found is that, Au_5 pathways have smaller activation energy for the first step involving hydrogen absorption of HCl to the nearby Au atom (0.01 eV). In the second and third steps, both Au_4 andAu_5 pathways have similar single step energy barriers.

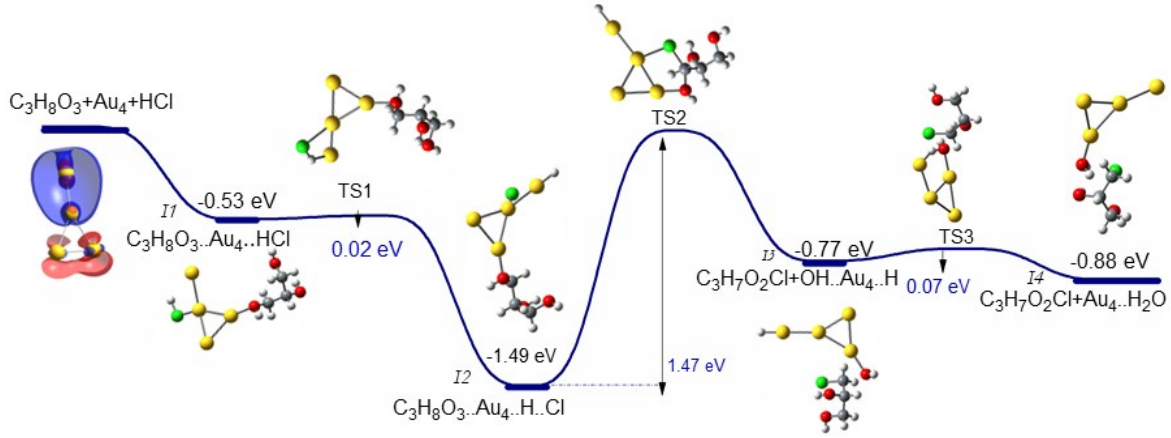

Figure S8. Reaction coordinates of '$C_3H_8O_3$+HCl+Au_n' involving conversion of $C_3H_8O_3$ to $C_3H_7O_2Cl$ over Au_4. Atoms in yellow, red, grey, white, green color represent Au, O, C, H and Cl respectively.

S6. FMO Analysis:

Table S1. Summary of Natural Population Analysis for $C_3H_8O_3$-Au_5-HCl complex.

			Natural Population			
Atom	No	Natural Charge	Core	Valence	Rydberg	Total
Au	1	-0.06936	33.99363	5.56219	0.01354	39.56936
Au	2	-0.25139	33.99518	5.74397	0.01224	39.75139
Au	3	0.03609	33.99350	5.45712	0.01329	39.46391
Au	4	-0.25147	33.99381	5.73804	0.01962	39.75147
Au	5	-0.15324	33.99570	5.65078	0.00676	39.65324
C	6	-0.02317	0.99949	2.01395	0.00973	3.02317
C	7	0.05237	0.99955	1.93619	0.01188	2.94763
C	8	-0.01605	0.99952	2.00656	0.00997	3.01605
O	9	-0.37077	0.99987	3.36383	0.00707	4.37077
O	10	-0.37161	0.99990	3.36520	0.00651	4.37161
O	11	-0.37657	0.99989	3.37228	0.00441	4.37657
H	12	0.26369	0.00000	0.23417	0.00214	0.23631
H	13	0.24541	0.00000	0.25185	0.00273	0.25459
H	14	0.23706	0.00000	0.26067	0.00227	0.26294
H	15	0.10047	0.00000	0.39810	0.00143	0.39953
H	16	0.09390	0.00000	0.40461	0.00149	0.40610
H	17	0.10175	0.00000	0.39616	0.00210	0.39825
H	18	0.08672	0.00000	0.41168	0.00160	0.41328
H	19	0.08317	0.00000	0.41509	0.00174	0.41683
Cl	20	-0.06875	4.99970	3.55563	0.01341	8.56875
H	21	0.15176	0.00000	0.34460	0.00364	0.34824
* Total *		-0.50000	180.96975	50.88267	0.14758	232.00000

Natural Population		
Effective Core	150.00000	
Core	30.96975	(99.9024% of 31)
Valence	50.88267	(99.7699% of 51)
Natural Minimal Basis	231.85242	(99.9364% of 232)
Natural Rydberg Basis	0.14758	(0.0636% of 232)

Table S2. Summary of Natural Population Analysis for $C_3H_8O_2Cl$-Au_5-HCl complex.

Atom	No	Natural Charge	Natural Population			
			Core	Valence	Rydberg	Total
C	1	-0.04223	1.99903	4.02156	0.02165	6.04223
C	2	0.11438	1.99908	3.86148	0.02507	5.88562
C	3	-0.37426	1.99889	4.35650	0.01888	6.37426
O	4	-0.74329	1.99976	6.72836	0.01518	8.74329
O	5	-0.77359	1.99978	6.76323	0.01059	8.77359
H	6	0.52594	0.00000	0.46882	0.00524	0.47406
H	7	0.48292	0.00000	0.51216	0.00492	0.51708
H	8	0.21255	0.00000	0.78532	0.00213	0.78745
H	9	0.20130	0.00000	0.79606	0.00264	0.79870
H	10	0.19337	0.00000	0.80298	0.00365	0.80663
H	11	0.21419	0.00000	0.78146	0.00435	0.78581
H	12	0.21447	0.00000	0.78013	0.00540	0.78553
Cl	13	-0.07436	9.99972	7.05440	0.02024	17.07436
Au	14	-0.02558	67.98762	11.01253	0.02543	79.02558
Au	15	-0.13176	67.98789	11.12194	0.02194	79.13176
Au	16	0.18280	67.98820	10.80527	0.02373	78.81720
Au	17	-0.27922	67.98698	11.25976	0.03248	79.27922
Au	18	-0.08991	67.99048	11.08785	0.01158	79.08991
Cl	19	-0.11987	9.99940	7.09538	0.02509	17.11987
H	20	0.31216	0.00000	0.68167	0.00617	0.68784
* Total *		0.00000	369.93681	100.77683	0.28635	471.00000

	Natural Population	
Effective Core	300.00000	
Core	69.93681	(99.9097% of 70)
Valence	100.77683	(99.7790% of 101)
Natural Minimal Basis	470.71365	(99.9392% of 471)
Natural Rydberg Basis	0.28635	(0.0608% of 471)

Table S3. Summary of Natural Population Analysis for $C_3H_8O_3$-Au_4-HCl complex.

			Natural Population			
Atom	No	Natural Charge	Core	Valence	Rydberg	Total
Au	1	-0.33797	67.99325	11.33714	0.00757	79.33797
Au	2	0.20288	67.99126	10.78025	0.02561	78.79712
Au	3	-0.35314	67.99328	11.33511	0.02475	79.35314
Au	4	0.15563	67.98932	10.84249	0.01256	78.84437
C	5	-0.04113	1.99909	4.02107	0.02097	6.04113
C	6	0.11224	1.99911	3.86429	0.02435	5.88776
C	7	-0.05554	1.99905	4.03332	0.02317	6.05554
O	8	-0.77334	1.99978	6.76409	0.00947	8.77334
O	9	-0.74909	1.99979	6.73963	0.00967	8.74909
O	10	-0.73908	1.99976	6.72342	0.01590	8.73908
H	11	0.48006	0.00000	0.51551	0.00443	0.51994
H	12	0.47355	0.00000	0.52079	0.00566	0.52645
H	13	0.52246	0.00000	0.47277	0.00477	0.47754
H	14	0.17152	0.00000	0.82546	0.00301	0.82848
H	15	0.17138	0.00000	0.82511	0.00351	0.82862
H	16	0.19327	0.00000	0.80357	0.00315	0.80673
H	17	0.20468	0.00000	0.79189	0.00343	0.79532
H	18	0.19107	0.00000	0.80578	0.00315	0.80893
Cl	19	-0.13813	9.99942	7.11330	0.02542	17.13813
H	20	0.30867	0.00000	0.68532	0.00600	0.69133
* Total *		-0.00000	293.96313	89.80033	0.23655	384.00000

Natural Population		
Effective Core	240.00000	
Core	53.96313	(99.9317% of 54)
Valence	89.80033	(99.7781% of 90)
Natural Minimal Basis	383.76345	(99.9384% of 384)
Natural Rydberg Basis	0.23655	(0.0616% of 384)

Table S4. Summary of Natural Population Analysis for $C_3H_8O_2Cl$-Au_4-HCl complex

Atom	No	Natural Charge	Natural Population			
			Core	Valence	Rydberg	Total
Au	1	-0.42000	67.99376	11.41895	0.00728	79.42000
Au	2	0.21930	67.99087	10.76402	0.02581	78.78070
Au	3	-0.32996	67.99328	11.31775	0.01893	79.32996
Au	4	0.21214	67.98948	10.78651	0.01187	78.78786
C	5	-0.37700	1.99889	4.35941	0.01870	6.37700
C	6	0.11736	1.99908	3.85798	0.02557	5.88264
C	7	-0.05120	1.99905	4.02943	0.02272	6.05120
O	8	-0.74304	1.99979	6.73279	0.01046	8.74304
O	9	-0.73745	1.99976	6.72247	0.01523	8.73745
H	10	0.47041	0.00000	0.52396	0.00563	0.52959
H	11	0.52521	0.00000	0.47029	0.00450	0.47479
H	12	0.21810	0.00000	0.77786	0.00404	0.78190
H	13	0.19418	0.00000	0.80176	0.00407	0.80582
H	14	0.20166	0.00000	0.79514	0.00320	0.79834
H	15	0.20023	0.00000	0.79675	0.00302	0.79977
Cl	16	-0.14799	9.99943	7.12106	0.02749	17.14799
H	17	0.30916	0.00000	0.68475	0.00609	0.69084
Cl	18	-0.06869	9.99972	7.04905	0.01993	17.06869
H	19	0.20760	0.00000	0.78754	0.00486	0.79240
* Total *		0.00000	301.96311	89.79750	0.23940	392.00000

	Natural Population	
Effective Core	240.00000	
Core	61.96311	(99.9405% of 62)
Valence	89.79750	(99.7750% of 90)
Natural Minimal Basis	391.76060	(99.9389% of 392)
Natural Rydberg Basis	0.23940	(0.0611% of 392)